Virchows Arch [Pathol Anat] (1982) 394:207–220

Virchows Archiv A

Erythrocytosis, Glomerulomegaly, Mesangial Hyperplasia, Sialyl Hyperplasia, and Arterioscleriosis Induced in Rats by Nickel Subsulfide *

Kilmer S. McCully, Lois A. Rinehimer, Concettina G. Gillies, Sidney M. Hopfer, and F. William Sunderman Jr

Departments of Laboratory Medicine, Pathology, and Pharmacology, University of Connecticut School of Medicine, 263 Farmington Avenue, Farmington, Connecticut 06032, USA

Summary. Histopathological examinations were performed upon groups of male Fischer rats killed at intervals from 1 h to 18 weeks after unilateral intrarenal (ir) injection of nickel subsulfide (2.5 or 5 mg of Ni_3S_2/rat). Consistent with previous findings, erythroid hyperplasia of bone marrow and spleen occurred from 2 to 18 weeks after Ni_3S_2-treatment, resulting in pronounced erythrocytosis. Hitherto unreported effects of Ni_3S_2-treatment include: (a) marked glomerulomegaly and hyperplasia of mesangial cells in both kidneys; (b) hyperplasia of submandibular salivary glands, and (c) widespread arteriosclerotic lesions. The present study suggests that mesangial cells of renal glomeruli produce erythropoietin. Discovery that ir injection of Ni_3S_2 induces arteriosclerotic lesions in rats furnishes a new experimental model to investigate the pathogenesis of arteriosclerosis.

Key words: Nickel subsulfide – Erythrocytosis – Mesangial hyperplasia – Sialyl hyperplasia – Arteriosclerosis

Introduction

Jasmin (1973) discovered that administration of nickel subsulfide (Ni_3S_2) to rats by intrarenal (ir) injection produces intense erythrocytosis after 1 month and malignant renal neoplasms after 8 months. These observations have been confirmed and extended in several subsequent studies (Jasmin and Solymoss 1975; Jasmin and Riopelle 1976; Jasmin 1978; Jasmin et al. 1979; Morse et al. 1977; Hopfer et al. 1978; Hopfer and Sunderman 1978; Sunderman et al. 1979; Oskarsson et al. 1981). Erythrocytosis induced by Ni_3S_2 is apparently mediated by enhanced production of erythropoietin, since erythropoietin activity is increased in serum of Ni_3S_2-treated rats (Solymoss and Jasmin 1978; Hopfer et al. 1979). Intramuscular or intrahepatic administration of Ni_3S_2 to rats does

* Supported by grants from the U.S. Department of Energy (EV-03140) and National Institute of Environmental Health Sicences (ES-01337)

Offprints requests to: F.W. Sunderman, Jr at the above address

0340-1227/82/0394/0207/$02.80

not affect erythropoiesis (Hopfer et al. 1980), although malignant tumors develop at the injection sites (Sunderman 1981). The present study was performed in order to identify the pathological reactions that occur in rats after ir administration of Ni_3S_2. In the present investigation, histopathologic examinations were performed upon groups of rats killed at intervals from 1 h to 18 weeks after unilateral ir injection of Ni_3S_2. Glomerulomegaly and mesangial hyperplasia occurred consistently in both kidneys of Ni_3S_2-treated rats. The Ni_3S_2-treated rats also developed erythroid hyperplasia in bone marrow and spleen, hyperplasia of submandibular salivary glands, and generalized arteriosclerosis.

Materials and Methods

Nickel subsulfide (αNi_3S_2, median particle diameter <2 μm) was provided by INCO Ltd., Toronto, Canada. Chemical and physical properties of the Ni_3S_2 and criteria of its purity have been described previously (Hopfer and Sunderman 1978). The experimental animals were 91 male rats of the Fischer 344 strain (Charles River Breeding Laboratories, Inc., Wilmington, MA, USA), which were approximately 2 months old at the time of intrarenal (ir) injection (mean body wt = 246 g, s.d. = 27 g). The rats were housed in stainless-steel cages and were fed Purina laboratory rat chow and water ad libitum. Injections of Ni_3S_2 (2.5 or 5 mg/rat) into the right kidney were performed as previously described (Morse et al. 1977; Hopfer et al. 1978). Control rats received similar injections of 0.2 ml of the vehicle. Blood samples (<80 μl) were obtained from each rat prior to ir injection and at biweekly or monthly intervals thereafter. The tip of the tail was incised with a scalpel, and blood was collected into heparinized capillary tubes for duplicate measurements of blood haematocrit, as described by Strumia et al. (1954).

Groups of Ni_3S_2-treated and control rats were killed by inhalation of diethyl ether at 6 intervals (1 h, 1 week, 2–3 weeks, 4 weeks, 8–10 weeks, and 18 weeks) after the ir injection. The brain, heart, kidneys, liver, and spleen were weighed. Histological sections of adrenal, aorta, bladder, bone (femur and sternum), brain, colon, duodenum, esophagus, heart, ileum, jejunum, kidneys (right and left), liver, lungs, lymph nodes (axillary and mesenteric), pancreas, seminal vesicle, spleen, stomach, submandibular salivary gland, testis, thymus, and trachea were fixed in 10% neutral buffered formalin. Paraffin-embedded sections were routinely stained with hematoxylin and eosin (H&E). Selected sections were stained by the periodic acid Schiff (PAS), van Gieson, Gomori silver reticulin, PAS-methenamine silver, and Prussian blue reactions. Smears of femoral bone marrow were stained with Wright's stain, and 100 marrow cells were counted to compute the myeloid/erythroid ratio.

Blocks of both kidneys of 8 Ni_3S_2-treated and 4 control rats, autopsied at 18 weeks after ir injection, were fixed in cacodylate buffered 4% glutaraldehyde, post-fixed in cacodylate buffered 2% osmium tetroxide, and embedded in epoxy resin for ultrathin sectioning. The sections were stained with toluidine blue for light microscopy, or with lead citrate and uranyl acetate for examination with a Phillips 300 electron microscope at 60 kV. Representative glomeruli and tubules in each kidney were photographed at 3,000×, 8,000×, and 17,000× magnification.

Mean glomerular volumes of kidneys from 69 rats (44 Ni_3S_2-treated rats and 25 controls) were computed from measurements of maximum glomerular diameter by means of a calibrated ocular micrometer. Twenty consecutive glomeruli in each kidney were measured, including subcapsular, cortical, and juxta-medullary glomeruli, and the mean glomerular volume was calculated, assuming spherical shape, using the equation $V = 4/3\ \pi r^3$. The average number of mesangial cells per glomerulus in both kidneys from 12 rats (8 Ni_3S_2-treated and 4 controls), autopsied at 18 weeks, was determined by light microscopy of 6 to 10 glomeruli in each kidney at 1,000× magnification, using ultrathin sections stained with toluidine blue. In addition, the average number of mesangial cells per low power field was determined by electron microscopy of several glomeruli in each kidney at 3,000× magnification.

Variances of haematocrits, myeloid/erythroid ratios, glomerular volumes, and mesangial cell counts were expressed as standard deviations (s.d.); the significance of differences between mean values in Ni_3S_2-treated and control rats was determined by Student's "t" test (when $n > 12$) and by the Mann-Whitney "U" test (when $n < 13$). The significance of differences between proportions

was computed by Fisher's exact text (when $n<70$) and by Chi-square test with Yates's correction (when $n>69$). Two-tailed estimates of probability were used for statistical tests; computations were performed according to Siegel (1956).

Results

In rats killed at 1 h after ir injection of Ni_3S_2, hematomas containing abundant Ni_3S_2 particles are present in the cortex and medulla of the injected right kidney. Scattered Ni_3S_2 particles are also seen in the non-injected left kidney, and in capillaries or sinusoids of the spleen, liver, lymph nodes, bone marrow, lungs, and adrenals. At 1 week, Ni_3S_2 particles remain along the needle tract in the injected kidney, and are readily apparent in glomerular mesangial cells of both kidneys, in splenic red pulp macrophages, in bone marrow macrophages, in lung capillaries, and in adrenal sinusoids. The quantity of Ni_3S_2 particles at these sites diminishes steadily during 10 weeks after the ir injection; by 18 weeks Ni_3S_2 particles are no longer detectable, even at the injection site.

Fibroblastic proliferation is noted along the needle tract in the right kidney at 1 week after ir injection of Ni_3S_2; it increases in intensity until, at 18 weeks, there is a prominent capsular scar composed of fibrous tissue with abundant collagen and reticulin fibers. Scattered infiltrates of lymphocytes, macrophages, and rare giant cells are seen in the parenchyma at the injected kidney at 4 to 18 weeks, as well as foci of fibrosis, calcification and hemosiderin deposition. Renal glomeruli adjacent to the needle tract are more hypercellular than those elsewhere in the injected kidney or in the opposite kidney. There is no evidence of neoplasia in the injected kidneys.

Erythrocytosis begins to develop at 2 weeks and is most pronounced at 8 weeks after ir injection of Ni_3S_2 (Fig. 1). For example, in rats that receive 2.5 mg or 5.0 mg of Ni_3S_2, the mean haematocrits at 8 weeks are 77% (s.d. = 6%) and 77% (s.d. = 1%), respectively, versus a mean haematocrit of 49% (s.d. = 1%) in controls ($P<0.001$). In rats killed at 18 weeks after ir injection of 2.5 mg of Ni_3S_2, the mean haematocrit is 76% (s.d. = 2%) ($P<0.001$ versus 50% (s.d. = 2%) in controls). Erythroid hyperplasia in bone marrow and spleen is evident at 2 weeks and becomes intense at 4 to 18 weeks. In 16 rats killed at 18 weeks after ir injection of Ni_3S_2 (2.5 mg), the myeloid/erythroid ratio in femoral

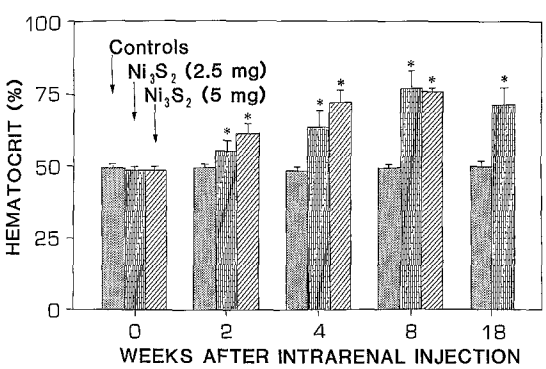

Fig. 1. Blood haematocrit values (%) in 12 controls, 16 Ni_3S_2-treated rats (2.5 mg/rat), and 6 Ni_3S_2-treated rats (5 mg/rat). The bars indicate the mean haematocrit values at specified intervals after ir injection of vehicle or Ni_3S_2. Vertical lines above the bars indicate ± 1 standard deviation. *Asterisks* indicate $P<0.01$ versus the corresponding value in controls, computed by Student's *t*-test

Table 1. Body weights and organ weights of rats killed at 18 weeks after intrarenal injection of vehicle or Ni_3S_2 (2.5 mg/rat). Mean values (g) ± 1 standard deviation are given

Parameter	Controls ($n=12$)	Ni_3S_2-Treated rats ($n=16$)	Student's *t*-test
Body weight	356 ±26	349 ±21	N.S.
Liver weight	11.7 ± 0.7	11.3 ± 1.1	N.S.
Brain weight	1.92± 0.87	1.91± 0.88	N.S.
Heart weight	1.04± 0.09	1.13± 0.14	$P<0.05$
Spleen weight	0.62± 0.05	1.01± 0.21	$P<0.01$
Right kidney weight	1.14± 0.11	1.29± 0.13	$P<0.01$
Left kidney weight	1.16± 0.11	1.37± 0.14	$P<0.01$

bone marrow averages 0.53 (s.d. = 0.52) ($P<0.001$ versus the corresponding M/E ratio of 3.2 (s.d. = 2.2) in 12 controls). Extramedullary haematopoiesis in the spleen results in splenomegaly. The mean weights of spleen, heart, and both kidneys are significantly greater in Ni_3S_2-treated rats at 18 weeks than in the corresponding controls (Table 1).

Glomerular morphology in kidneys of Ni_3S_2-treated rats is illustrated in Fig. 2a–d, 3a and b, and 4. Hyperplasia of mesangial cells is prominent in both kidneys of Ni_3S_2-treated rats at 1 to 18 weeks after ir injection. Occasional mesangial cells in mitosis are seen during this period. The mean glomerular volume becomes significantly increased from 4 to 18 weeks (Table 2). The number of mesangial cells in glomeruli of rats killed at 18 weeks after ir injection of Ni_3S_2 is approximately twice the corresponding number in control rats (Table 3). The mean glomerular volumes and mesangial cell counts are increased to the same degree in the non-injected left kidneys as in the injected right kidneys of Ni_3S_2-treated rats. Hyperplastic mesangial cells occur in clusters within glomerular lobules and extend to the base of the vascular tuft, where they surround afferent and efferent arterioles. The hyperplastic mesangial cells have moderately hyperchromatic oval or indented nuclei, and increased amount of cytoplasm, which is eosinophilic, PAS-positive, and argyrophilic. Electron microscopy shows that the mesangial cells contain abundant mesangial matrix, rough endoplasmic reticulum, free ribosomes, microtubules, microfilaments, and Golgi apparatus. Glomerular basement membranes, endothelial cells, parietal epithelial cells, juxtaglomerular cells and tubular lining cells are all normal.

Pronounced hyperplasia of the submandibular salivary gland occurs at 1 week following ir injection of Ni_3S_2 and persists throughout the period of observation (Fig. 3c and d). Peri-acinar cells of the salivary gland are increased in number and are moderately hyperchromatic. The nuclei of acinar cells are also hyperchromatic and occasionally are doubled. At 4–10 weeks, mitoses are frequently seen in peri-acinar and acinar cells, and secretory activity of the salivary gland appears to be diminished.

Widespread arteriosclerotic lesions are found in the aorta and in arteries and arterioles of the heart, kidneys, brain, lungs, and other organs following ir injection of Ni_3S_2 (Table 4 and Fig. 5a–d). Characteristic fibrous intimal plaques, consisting of hyperplastic smooth muscle cells, deposition of edematous ground substance, and splitting of elastic fibers are identified. These lesions

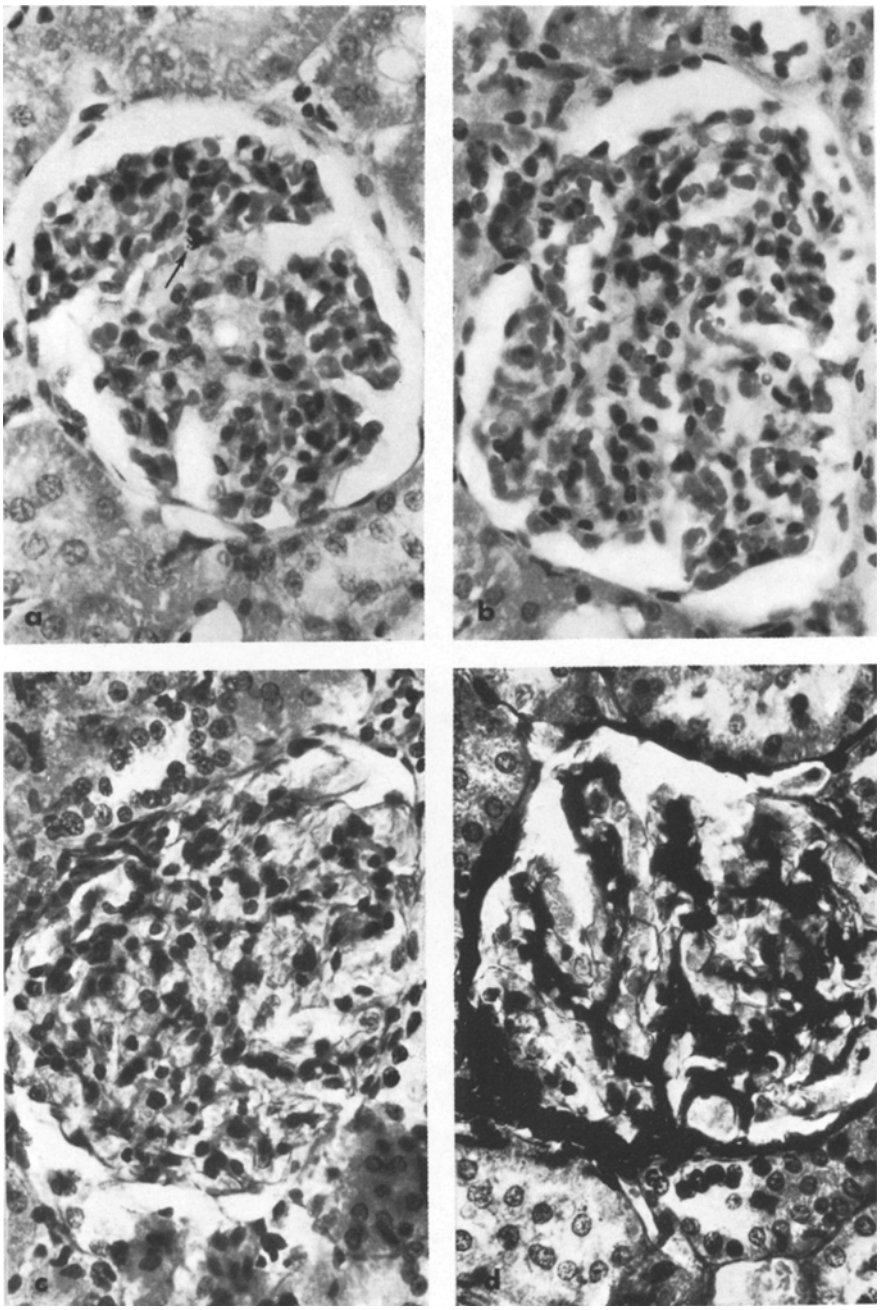

Fig. 2a–d. Photomicrographs of renal glomeruli at specified intervals after ir injection of Ni_3S_2 (2.5 mg/rat). **a** Mesangial cell hyperplasia, at 4 weeks. One mesangial cell contains Ni_3S_2 particles (arrow) (H&E, 300×). **b** Glomerular enlargement and congestion with mesangial hyperplasia, at 4 weeks (H&E, 300×). **c** Glomerulomegaly with mesangial hyperplasia and abundant deposits of mesangial matrix, at 18 weeks (PAS, 300×). **d** Deposits of argyrophilic mesangial matrix, at 18 weeks. (PAS-methenamine silver, 300×)

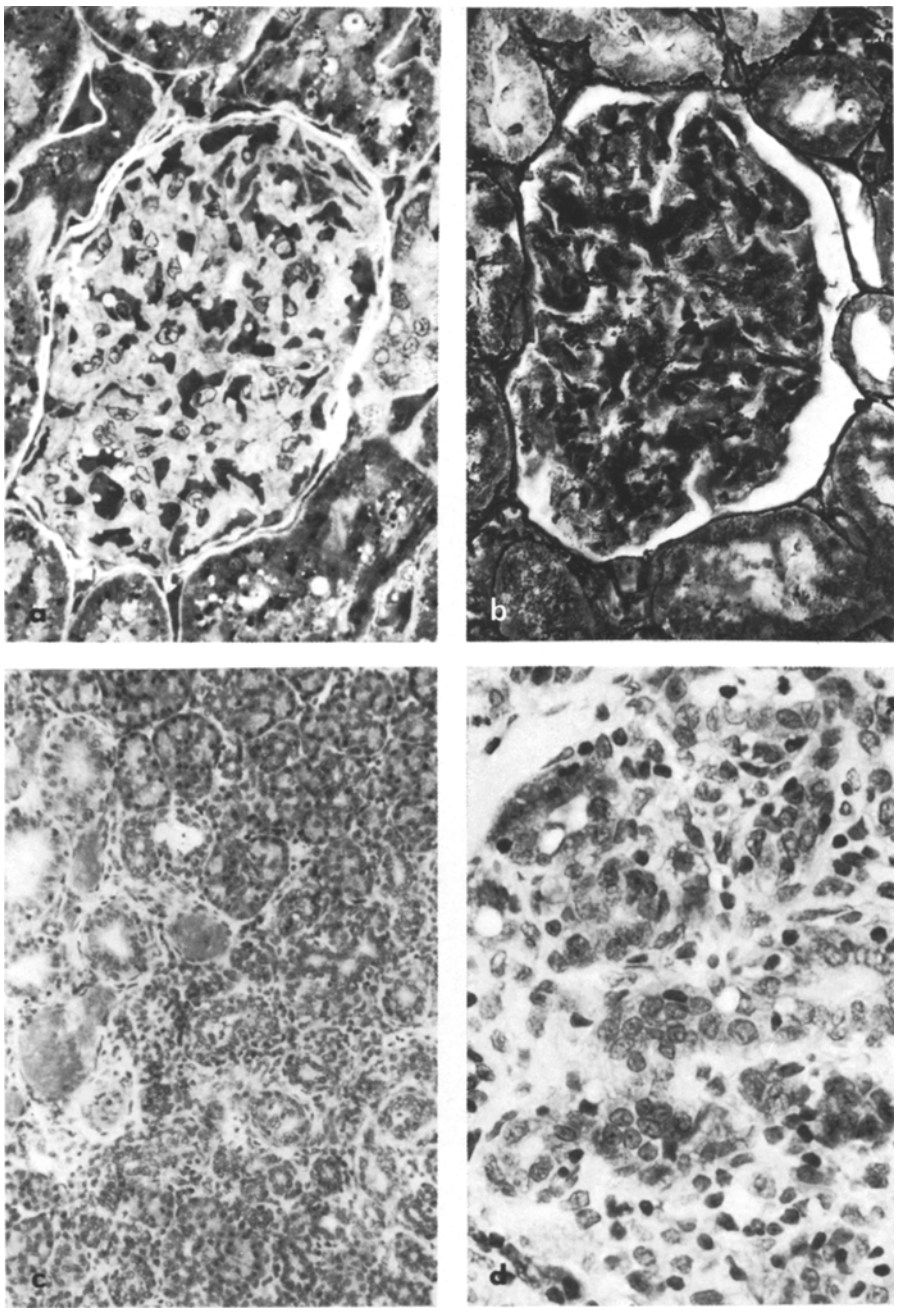

Fig. 3a–d. Photomicrographs of renal glomeruli and submandibular salivary glands at specified intervals after ir injection of Ni_3S_2 (2.5 or 5 mg/rat). **a** Mesangial hyperplasia and deposits of mesangial matrix in glomerulus, at 18 weeks (2.5 mg Ni_3S_2/rat). (Ultrathin epoxy section, toluidine blue, 300×). **b** Granular, argyrophilic, mesangial matrix in glomerulus, at 18 weeks (2.5 mg Ni_3S_2/rat). (Gomori reticulin, 300×). **c** Submandibular gland, with hyperplasia of acinar and peri-acinar cells, at 8 weeks (5 mg Ni_3S_2/rat). (H&E, 50×). **d** Submandibular gland with sialyl hyperplasia, at 8 weeks (5 mg Ni_3S_2/rat). (H&E, 300×)

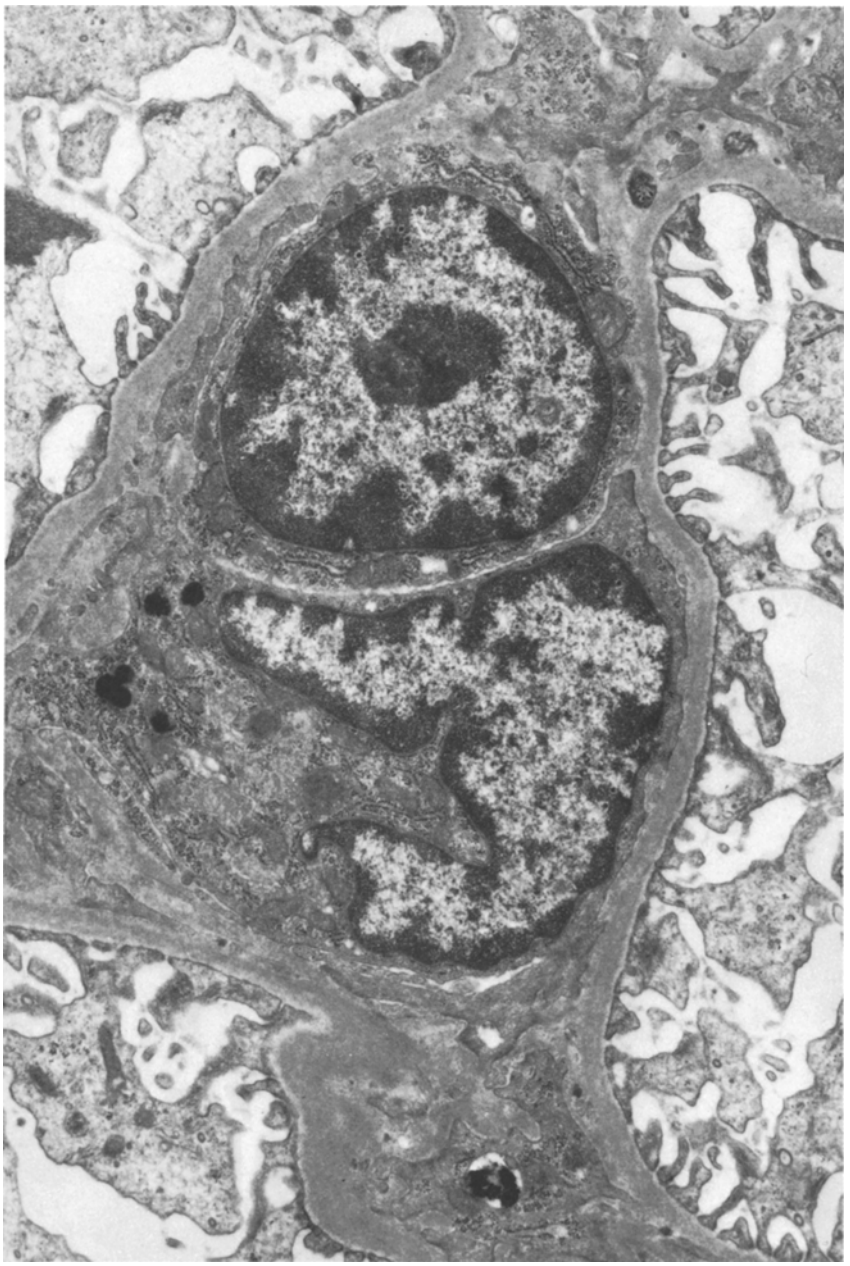

Fig. 4. Electron micrograph of renal glomerulus at 18 weeks after ir injection of Ni_3S_2 (2.5 mg/rat). Hyperplastic mesangial cells contain prominent ribosomes and are surrounded by abundant mesangial matrix. (Lead citrate/uranyl acetate, 13,000 ×)

Table 2. Glomerular volumes of control and Ni_3S_2-treated rats at specified intervals after intrarenal injection. Maximum diameters of 40 renal glomeruli of each rat were measured by ocular micrometry and glomerular volumes were estimated by the equation $V=4/3\,\pi r^3$. Each entry represents the mean value ($\mu m^3 \times 10^6$) $\pm$ 1 standard deviation for the number of rats that is listed within parentheses. No significant differences were observed between the mean glomerular volumes of right kidneys versus left kidneys in any of the treatment groups at any of the specified intervals

Ni_3S_2 dosage (mg/rat)	1 h	1 week	2–3 weeks	4 weeks	8–10 weeks	18 weeks	2–18 weeks
0	0.74 ± 0.12 (3)	0.64 ± 0.13 (5)	0.85 ± 0.12 (5)	0.87 ± 0.12 (5)	0.93 ± 0.09 (3)	1.01 ± 0.05 (4)	0.90 ± 0.11 (17)
2.5	0.68 ± 0.09 (3)	0.77 ± 0.14 (3)	1.10 ± 0.19 (6)	1.30 ± 0.26* (6)	1.72 ± 0.33* (6)	1.44 ± 0.24* (4)	1.37 ± 0.34** (22)
5	0.69 ± 0.04 (3)	0.70 ± 0.04 (3)	0.92 ± 0.08 (3)	1.12 ± 0.09* (3)	1.29 ± 0.09* (4)		1.11 ± 0.17** (10)

* $P<0.05$ versus corresponding value in controls, computed by Mann-Whitney U-test
** $P<0.01$ versus corresponding value in controls, computed by Student's t-test

Table 3. Indices of mesangial cellularity in glomeruli of rats killed at 18 weeks after intrarenal injection of vehicle or Ni_3S_2 (2.5 mg/rat). Mesangial cell indices are given as mean values ± 1 standard deviation

Parameter	Controls ($n=4$)	Ni_3S_2-Treated rats ($n=8$)	Mann-Whitney U-test
Mesangial cell counts by light microscopy (mesangial cells/glomerulus)			
Right kidney	15.4 ± 6.0	35.3 ± 7.9	$P<0.01$
Left kidney	18.5 ± 3.8	37.2 ± 7.7	$P<0.01$
Both kidneys	16.7 ± 5.1	35.5 ± 7.9	$P<0.01$
Mesangial cell counts by electron microscopy (mesangial cells/field at 3,000×)			
Right kidney	4.3 ± 0.9	10.0 ± 4.8	$P<0.05$
Left kidney	4.0 ± 2.1	8.0 ± 3.8	$P<0.05$
Both kidneys	4.3 ± 1.6	8.8 ± 4.3	$P<0.05$

are found in half of the rats killed at 1 week after ir injection of Ni_3S_2, and they increase in number and intensity with time, until they are found in 39 of 43 Ni_3S_2-treated rats (91%) killed between 2 and 18 weeks, versus corresponding lesions in 6 of 28 control rats (21%), ($P<0.001$, computed by Chi-square test). Focal necrosis of arterial media adjacent to fibrous plaques is seen in a few rats at 2 to 4 weeks after ir injection of Ni_3S_2 and in 6 of 9 rats in the 8–10 week groups. Mural thrombi, partially occluding the lumen, are associated with fibrous intimal plaques in 2 of these rats. Vacuolization and hyperplasia of endothelial cells occur in most Ni_3S_2-treated rats from

Table 4. Arteriosclerotic lesions in control and Ni_3S_2-treated rats, from light microscopy of heart, kidneys, brain, aorta, and lungs. Each entry gives the incidence of lesions in rats killed at the specified intervals after intrarenal injection

Lesion	Ni_3S_2 Dosage (mg/rat)	1 h	Weeks					
			1	2–3	4	8–10	18	2–18
Endothelial	0	1/3	0/5	2/5	1/5	0/3	0/15	3/28
hyperplasia	2.5	2/3	1/3	6/6	5/6	5/6*	0/16	16/34**
and vacuolization	5	1/3	3/3	3/3	3/3	2/3		8/9**
Subintimal edema	0	2/3	0/5	1/5	1/5	2/3	1/15	5/28
with splitting	2.5	3/3	2/3	5/6*	6/6*	6/6	10/16**	27/34**
of elastica	5	1/3	1/3	3/3	3/3	3/3		9/9**
Fibrous intimal	0	0/3	0/5	0/5	0/5	0/3	6/15	6/28
plaques	2.5	0/3	2/3	5/6*	6/6*	5/6*	15/16**	31/34**
	5	1/3	1/3	2/3	3/3*	3/3*		8/9**
Focal medial	0	0/3	0/5	0/5	0/5	0/3	0/15	0/28
necrosis next	2.5	0/3	0/3	1/6	1/6	4/6***	0/16	6/34*
to fibrous plaque	5	1/3	0/3	0/3	0/3	2/3		2/9

* P 0.05 versus controls, computed by Fisher's exact test
** P 0.01 versus controls, computed by Fisher's exact test
*** Two rats with focal medial necrosis also had mural thrombosis

2 to 10 weeks, and in a few controls (Table 4). Subintimal edema and focal splitting of the internal elastic membrane, but without smooth muscle cell hyperplasia and other characteristic features of fibrous plaques, are observed in most Ni_3S_2-treated rats and in a few controls.

No other consistent, significant, or unusual histopathologic lesions are observed in the Ni_3S_2-treated and control rats. No benign or malignant neoplasms are identified in any of the rats.

Discussion

Intrarenal injection of Ni_3S_2 produces widespread embolization of Ni_3S_2 particles within blood vessels of the major organs. Phagocytic cells of liver, spleen, bone marrow, kidneys, lymph nodes, and adrenals contain Ni_3S_2 particles in a pattern similar to that seen after injection of carbon particles (Benacerraf et al. 1959). Mesangial cells in glomeruli of both kidneys avidly phagocytize Ni_3S_2 particles in a manner similar to that reported after iv injection of carbon particles (Grond et al. 1980). Hyperplasia of mesangial cells begins within 1 week after ir injection of Ni_3S_2 and continues for 18 weeks, not only in the injected kidney but in the opposite kidney as well. Glomerulomegaly is evident at 4 weeks, and continues to develop in association with mesangial hyperplasia; glomerulomegaly is maximal at 8 to 10 weeks. Mesangial cell hyperplasia and glomerulomegaly parallel the development of erythrocytosis in Ni_3S_2-treated rats.

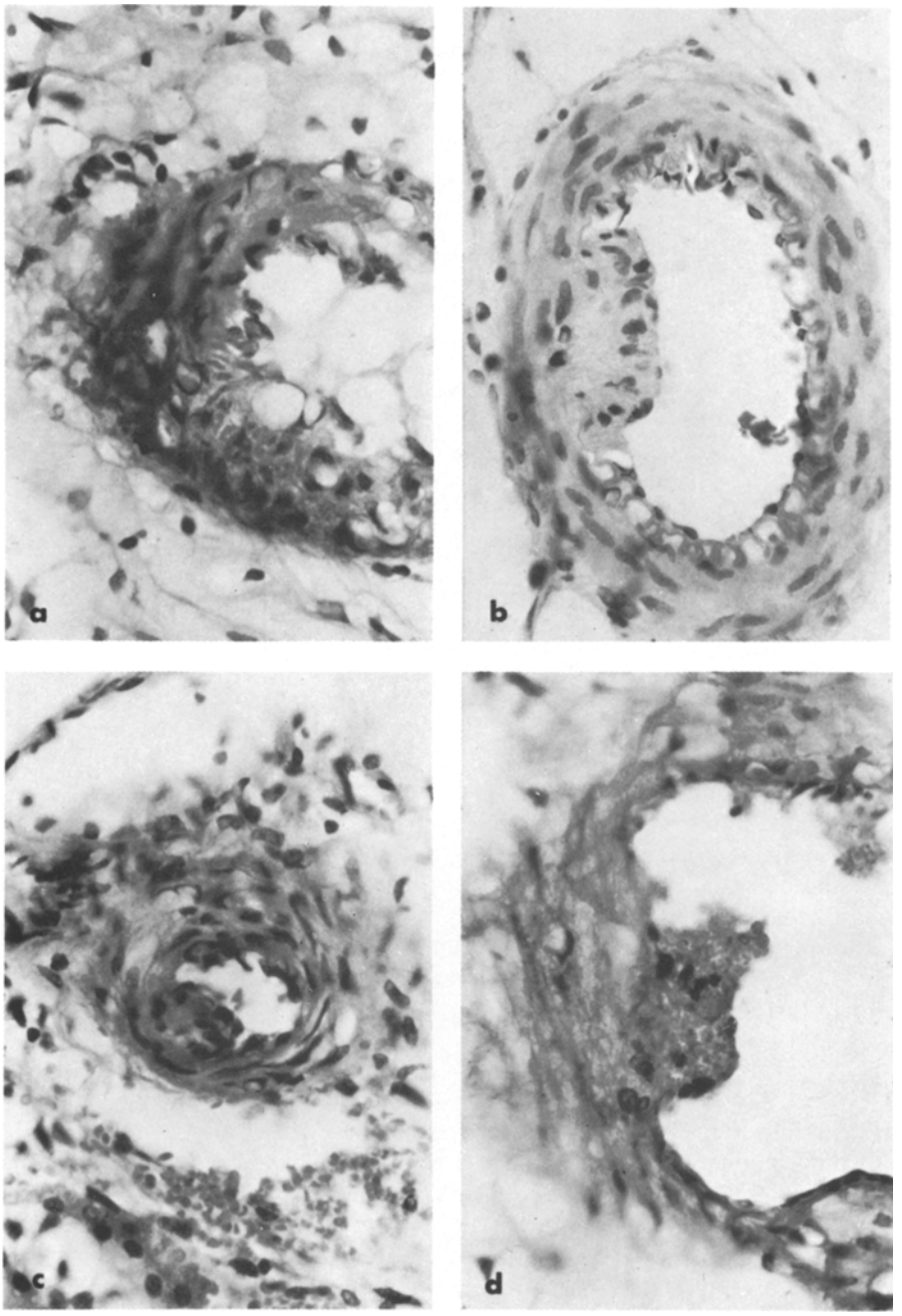

Fig. 5a–d. Photomicrographs of arteries and arterioles at specified intervals after ir injection of Ni_3S_2 (2.5 mg/rat). **a** Renal arteriole with focal medial necrosis and medial hemorrhage, at 8 weeks. (H&E, 300×). **b** Cerebral artery narrowed by fibrous plaque consisting of hyperplasic smooth muscle cells, deposition of ground substance, and splitting of elastica interna, at 4 weeks. (H&E, 300×). **c** Renal arteriole narrowed by focal hyperplasia of smooth muscle cells and deposition of ground substance, with vacuolization of endothelial cells, at 4 weeks. (H&E, 300×). **d** Renal arteriole with focal medial necrosis and mural thrombosis, at 8 weeks. (H&E, 300×)

There is controversy over which type of renal cell produces erythropoietin (Gordon 1973; Fisher and Busuttil 1977). The hormone is apparently derived from the glomerulus, since anti-erythropoietin antibody stains glomeruli in man and experimental animals (Fisher et al. 1965; Frenkel et al. 1968; Busuttil et al. 1971 and 1972). The antibody staining of the glomerular tuft occurs within lobules (Fisher et al. 1965; Busuttil et al. 1971), is most intense at the periphery of the glomerulus (Busuttil et al. 1972), and "characteristically involves the periphery of the glomerulus in a crescent-like pattern" (Frenkel et al. 1968). This pattern is identical to the distribution of mesangial cells within the glomerular tuft, as observed in the present study. The parietal epithelial cells, juxtaglomerular cells, and renal tubular cells are not stained by anti-erythropoietin antibody (Busuttil et al. 1971), and these cells are all normal in the present study. Therefore, we speculate that mesangial cells may be responsible for erythropoietin production, at least in Ni_3S_2-treated rats.

The occurrence of mesangial cell hyperplasia and glomerulomegaly in human subjects with hypoxia and erythrocytosis supports the hypothesis that mesangial cells produce erythropoietin. Enlarged, hypercellular glomeruli with increased numbers of mesangial cells have been documented in patients with cyanotic congenital heart disease (Meesen and Litton 1953; Bauer and Rosenberg 1960; Spear 1960; Inglefinger et al. 1970). Eosinophilic, PAS-positive material is increased in the intercapillary region of glomeruli in these cases, resembling the accumulation of PAS-positive material in the present study. Mesangial cell hyperplasia also occurs in patients with chronic cor pulmonale (Ellis 1961), cystic fibrosis with hypoxia (Oppenheimer 1972), and chronic pulmonary hypertension (Cadillo 1962; Spear 1964). Moreover, glomerulomegaly and mesangial cell hyperplasia occur in association with erythrocytosis and increased erythropoietin production in experimental animals exposed to hypoxia (Highman and Altman 1949; Spear and Kihara 1972).

The histogenesis of renal neoplasms induced by ir injection of Ni_3S_2 (Jasmin and Riopelle 1976; Sunderman et al. 1979) may be clarified by comparisons of the tumor cells with the hyperplastic mesangial cells observed in the present study. The renal neoplasms appear sarcomatous, but possess certain features characteristic of epithelial tumors (Jasmin and Riopelle 1976). Further ultrastructural study is required to document whether or not these tumors may be derived from hyperplastic mesangial cells.

An original objective of this study was to investigate the microcrystalline inclusions that were reported by Jasmin (1978) and Jasmin et al. (1979) in mitochondria of tubular lining cells in the straight portion of the distal nephron of rats at 2 to 16 weeks after ir injection of Ni_3S_2 (10 mg/rat). In the present study, failure to find mitochondrial inclusions may be related to the lower doses of Ni_3S_2 that were used, or, more likely, to differences in the post-fixation technique for electron microscopy. Jasmin (1978) prepared 2% osmium tetroxide in barbital buffer solution (pH 7.2) containing 0.22 *M* sucrose, whereas cacodylate buffered osmium tetroxide (without sucrose) was employed in this study.

Sialyl hyperplasia was an unanticipated finding in the present study. Catalanatto and Sunderman (1977) and Hofsoy et al. (1979) showed that saliva is a significant excretory route for nickel in humans and rabbits, and Jacobsen

et al. (1977) reported that human submandibular gland contains secretory proteins with exceptional affinity for nickel. Since salivary gland has been identified as an extrarenal site of erythropoietin production (Zaugheri et al. 1973; Alvarez-Ugarte et al. 1976; Fava-de-Moraes et al. 1979), we speculate that erythropoietin production by peri-acinar cells of the salivary gland may contribute to Ni_3S_2-induced erythropoietinemia (Solymoss and Jasmin 1978; Hopfer et al. 1979).

Rats are notably resistant to experimental arteriosclerosis. The present discovery that ir injection of Ni_3S_2 induces widespread arteriosclerotic lesions in rats provides a new avenue to investigate the pathogenesis of arteriosclerosis. Experiments are in progress to ascertain whether or not intravenous injection of Ni_3S_2 also induces arteriosclerotic lesions in rats. There are few published studies of the effects of nickel compounds on blood vessels or lipid metabolism. Kovach et al. (1980) and Rubanyi and Kovach (1980) found that iv administration of $NiCl_2$ to dogs increases coronary artery resistance, reduces coronary blood flow, and depresses reactive dilatation of coronary vessels following episodes of myocardial ischemia. Clary (1975) observed that addition of $NiCl_2$ to rats' drinking water for 4 months produces hypocholesterolemia and hypotriglyceridemia. On the other hand, Manthur and Tandon (1979) observed that parenteral administration of $NiSO_4$ to rats, daily for 2 weeks, causes hypercholesterolemia and hyperphospholipidemia. The arteriosclerotic lesions that were induced by Ni_3S_2 in the present study mimic the lesions that follow parenteral or oral administration of homocysteine to various experimental animals (McCully and Ragsdale 1970; McCully and Wilson 1975; Harker et al. 1976; Hladovec 1979). Within 24 h, an iv injection of homocysteine produces widespread intimal damage, endothelemia, increased vascular permeability, platelet sequestration, and microthromboses. Mesangial cell hyperplasia is associated with arteriosclerosis in patients with hereditary enzymatic disorders of homocysteine metabolism (McCully 1969). Studies are underway in our laboratory to contrast the arterial lesions induced by Ni_3S_2 and homocysteine in rats, and to explore the interrelationships of nickel, methionine, and homocysteine metabolism that were suggested many years ago by Griffith et al. (1942).

References

Alvarez-Ugarte CA, Soriano G, Giglio JM, Bozzini, CE (1976) Effect of parasympathetic denervation or duct ligation of rat submandibular glands on extrarenal erythropoietin production. J Endocrinol 70:309–310

Bauer WC, Rosenberg BF (1960) A quantitative study of glomerular enlargement without an increase in renal mass. Am J Pathol 37:695–712

Benacerraf B, McCluskey RT, Patras D (1959) Localization of colloidal substance in vascular endothelium. A mechanism of tissue damage. Am J Pathol 35:75–91

Busuttil RW, Roh BL, Fisher JW (1971) The cytological localization of erythropoietin in the human kidney using the fluorescent antibody technique. Proc Soc Exp Biol Med 137:327–330

Busuttil RW, Roh BL, Fisher JW (1972) Localization of erythropoietin in the glomerulus of the hypoxic dog kidney using a fluorescent antibody technique. Acta Haematol 47:238–242

Cadillo M (1962) Alteraciones glomerulares en le hipertension pulmonar e hipertrofia ventricular derecha. An Fac Med Lima 45:3–21

Catalanatto FA, Sunderman FW Jr (1977) Nickel concentrations in human parotid saliva. Ann Clin Lab Sci 7:146–151

Clary JJ (1975) Nickel chloride-induced metabolic changes in the rat and guinea pig. Toxicol Appl Pharmacol 31:55–65

Ellis PA (1961) Renal enlargement in chronic cor pulmonale. J Clin Pathol 14:552–556
Fave-de-Moraes F, Zaugheri EO, Doine AT (1979) Immunohistochemical localization of erythropoietin in the rat and mouse submandibular gland. Histochem J 21:97–102
Fisher JW, Busuttil RW (1977) Sites of production of eryhtropoietin. In: Fisher JW (ed) Kidney hormones: Erythropoietin. Academic Press, New York, pp 165–185
Fisher JW, Taylor G, Porteus DD (1965) Localization of erythropoietin in glomeruli of sheep kidney by fluorescent antibody technique. Nature 205:611–612
Frenkel EP, Suki W, Baum J (1968) Some observations on the localization of erythropoietin. Ann NY Acad Sci 149:292–293
Gordon AS (1973) Erythropoietin. Vitam Horm 31:105–174
Griffith WH, Pavcek PL, Mulford DJ (1942) The relation of the sulfur amino acids to the toxicity of cobalt and nickel in the rat. J Nutr 23:603–612
Grond J, Daha MR, Elema JD (1980) Glomerular mesangial uptake of intravenously injected colloidal carbon in the rat determined by an image analyzing method: Lack of influence of platelet aggregation or complement activation. Virchows Arch [Cell Pathol] 33:281–291
Harker LA, Ross R, Slichter SJ, Scott CR (1976) Homocysteine-induced arteriosclerosis. Role of endothelial cell injury and platelet response to its genesis. J Clin Invest 58:731–741
Highman B, Altman PD (1949) Acclimatization response and pathological changes in rats at an altitude of 25,000 feet. Arch Pathol 48:503–515
Hladovec J (1979) Experimental homocysteinemia, endothelial lesions, and thrombosis. Blood Vessels 16:202–205
Hofsoy H, Paulsen G, Jonsen J (1979) Secretion of nickel in rabbit saliva. Ann Clin Lab Sci 9:479–486
Hopfer SM, Sunderman FW Jr (1978) Manganese inhibition of nickel subsulfide induction of erythrocytosis in rats. Res Commun Chem Pathol Pharmacol 19:337–345
Hopfer SM, Sunderman FW Jr, Fredrickson TN, Morse EE (1978) Nickel-induced erythrocytosis: Efficacies of nickel compounds and susceptibilities of rat strains. Ann Clin Lab Sci 8:396–402
Hopfer SM, Sunderman FW Jr, Fredrickson TN, Morse EE (1979) Increased serum erythropoietin activity in rats following intrarenal injection of nickel subsulfide. Res Commun Chem Pathol Pharmacol 23:155–170
Hopfer SM, Sunderman FW Jr, Morse EE, Fredrickson TN (1980) Effects of intrarenal injection of nickel subsulfide in rodents. Ann Clin Lab Sci 10:54–64
Inglefinger JR, Kissane JM, Robson AM (1970) Glomerulomegaly in a patient with cyanotic congenital heart disease. Am J Dis Child 120:69–71
Jacobsen N, Brennhovd I, Jonsen J (1977) Human submandibular gland tissue in culture. 2. Nickel affinity to secretory proteins. J Biol Buccale 5:169–175
Jasmin G (1973) Experimental production of polycythemia in rats with nickel sulfide. Clin Res 21:1068
Jasmin G (1978) Ultrastructural patterns of Ni-induced crystalline inclusions in mitochondria of renal tubules. Exp Mol Pathol 29:199–210
Jasmin G, Riopelle JL (1976) Renal carcinomas and erythrocytosis in rats following intrarenal injection of nickel subsulfide. Lab Invest 35:71–78
Jasmin G, Solymoss B (1975) Polycythemia induced in rats by intrarenal injection of nickel subsulfide, αNi_3S_2. Proc Soc Exp Biol Med 148:774–776
Jasmin G, Bouveau R, Andre J (1979) Etude par goniometrie des inclusion cristallines mitochondriales induites par le subsulfure de nickel chez le rat. Biol Cell 31:18–88
Kovach AGB, Rubanyi G, Ligeti L, Koller A (1980) Reduction of coronary and hind limb blood flow and reactive hyperaemia in dogs caused by nickel chloride. In: Brown SS, Sunderman FW Jr (eds) Nickel toxicology. Academic Press, New York, pp 137–140
McCully KS (1969) Vascular pathology of homocysteinemia: Implications for the pathogenesis of arteriosclerosis. Am J Pathol 56:111–128
McCully KS, Ragsdale BD (1970) Production of arteriosclerosis by homocysteinemia. Am J Pathol 61:1–11
McCully KS, Wilson RB (1975) Homocysteine theory of arteriosclerosis. Atherosclerosis 22:215–227
Manthur AK, Tandon SK (1979) Some biochemical alterations in early nickel toxicity. Chemosphere 11:893–901
Meesen H, Litton MA (1953) Morphology of the kidney in morbus caeruleus. Arch Pathol 56:480–487

Morse EE, Lee-T-Y, Reiss RF, Sunderman FW Jr (1977) Dose-response and time-response study of erythrocytosis in rats after intrarenal injection of nickel subsulfide. Ann Clin Lab Sci 7:17–24

Oppenheimer EA (1972) Glomerular lesions in cystic fibrosis: possible relation to diabetes mellitus, acquired cyanotic heart disease, and cirrhosis of the liver. Johns Hopkins Med J 131:351–366

Oskarsson A, Reid MC, Sunderman FW Jr (1981) Effects of cobalt chloride, nickel chloride, and nickel subsulfide upon erythropoiesis in rats. Ann Clin Lab Sci 11:165–172

Rubanyi G, Kovach AGB (1980) Cardiovascular actions of nickel ions. Acta Physiol Acad Sci Hung 55:345–353

Siegel S (1956) Nonparametric statistics for the behavioral sciences. McGraw-Hill Book Co., New York, pp 1–312

Solymoss B, Jasmin G (1978) Studies on the mechanism of polycythemia induced in rats by Ni_3S_2. Exp Hemat 6:43–47

Spear GS (1960) Glomerular alterations in cyanotic congenital heart disease. Bull Johns Hopkins Hosp 106:347–367

Spear GS (1964) The glomerulus in cyanotic congenital heart disease and primary pulmonary hypertension. A review. Nephron 1:238–248

Spear GS, Kihara I (1972) The glomerulus and serum sickness in experimental hypoxia. Br J Exp Pathol 53:265–276

Strumia MM, Sample AB, Hart ED (1954) An improved micro hematocrit method. Am J Clin Pathol 24:1016–1024

Sunderman FW Jr (1981) Recent research on nickel carcinogenesis. Envir Health Persp 40:131–141

Sunderman FW Jr, Maenza RM, Hopfer SM, Mitchell JM, Allpass PR, Damjanov I (1979) Induction of renal cancers in rats by intrarenal injection of nickel subsulfide. J Environ Pathol Toxicol 2:1511–1527

Zaugheri EO, Fava-de-Moraes F, Lopez OI, Marias I (1973) The role of submandibular glands on extra-renal erythropoietin production. Experientia 29:706–707

Accepted October 2, 1981